JCI The Journal of Clinical Investigation

Differential impact of prostaglandin H synthase 1 knockdown on platelets and parturition

Ying Yu, … , Garret A. FitzGerald, Colin D. Funk

J Clin Invest. 2005;115(4):986-995. https://doi.org/10.1172/JCI23683.

Article **Cardiology**

Platelet activation is a hallmark of severe preeclampsia, and platelet PGH synthase 1–derived (PGHS1-derived) thromboxane A_2 (TxA_2) has been implicated in its pathogenesis. However, genetic disruption of PGHS1 delays parturition. We created hypomorphic PGHS1 ($PGHS1^{Neo/Neo}$) mice, in which the substantial but tissue-dependent variability in the inhibition of PGHS1-derived eicosanoids achieved by low-dose aspirin treatment is mimicked, to assess the relative impact of this strategy on hemostatic and reproductive function. Depression of platelet TxA_2 by 98% in $PGHS1^{Neo/Neo}$ mice decreased platelet aggregation and prevented thrombosis. Similarly, depression of macrophage PGE_2 by 75% was associated with selectively impaired inflammatory responses. $PGF_{2\alpha}$ at 8% WT levels was sufficient to induce coordinated temporal oxytocin receptor (OTR) expression in uterus and normal ovarian luteolysis in $PGHS1^{Neo/Neo}$ mice at late gestation, while absence of PGHS1 expression in null mice delayed OTR induction and the programmed decrease of serum progesterone during parturition. Thus, extensive but tissue-dependent variability in PG suppression, as occurs with low-dose aspirin treatment, prevents thrombosis and impairs the inflammatory response but sustains parturition. $PGHS1^{Neo/Neo}$ mice provide a model of low-dose aspirin therapy that elucidates how prevention or delay of preeclampsia might be achieved without compromising reproductive function.

Differential impact of prostaglandin H synthase 1 knockdown on platelets and parturition

Ying Yu,[1] Yan Cheng,[1] Jinjin Fan,[1] Xin-Sheng Chen,[1] Andres Klein-Szanto,[2] Garret A. FitzGerald,[1] and Colin D. Funk[1,3]

[1]Institute for Translational Medicine and Therapeutics, University of Pennsylvania, Philadelphia, Pennsylvania, USA. [2]Fox Chase Cancer Center, Philadelphia, Pennsylvania, USA. [3]Departments of Physiology and Biochemistry, Queen's University, Kingston, Ontario, Canada.

Platelet activation is a hallmark of severe preeclampsia, and platelet PGH synthase 1–derived (PGHS1-derived) thromboxane A_2 (TxA_2) has been implicated in its pathogenesis. However, genetic disruption of PGHS1 delays parturition. We created hypomorphic PGHS1 ($PGHS1^{Neo/Neo}$) mice, in which the substantial but tissue-dependent variability in the inhibition of PGHS1-derived eicosanoids achieved by low-dose aspirin treatment is mimicked, to assess the relative impact of this strategy on hemostatic and reproductive function. Depression of platelet TxA_2 by 98% in $PGHS1^{Neo/Neo}$ mice decreased platelet aggregation and prevented thrombosis. Similarly, depression of macrophage PGE_2 by 75% was associated with selectively impaired inflammatory responses. $PGF_{2\alpha}$ at 8% WT levels was sufficient to induce coordinated temporal oxytocin receptor (OTR) expression in uterus and normal ovarian luteolysis in $PGHS1^{Neo/Neo}$ mice at late gestation, while absence of PGHS1 expression in null mice delayed OTR induction and the programmed decrease of serum progesterone during parturition. Thus, extensive but tissue-dependent variability in PG suppression, as occurs with low-dose aspirin treatment, prevents thrombosis and impairs the inflammatory response but sustains parturition. $PGHS1^{Neo/Neo}$ mice provide a model of low-dose aspirin therapy that elucidates how prevention or delay of preeclampsia might be achieved without compromising reproductive function.

Introduction

PGH synthase (PGHS) is a key enzyme required for conversion of arachidonic acid (AA) to PGH_2 for subsequent metabolism by individual PG synthases to generate PGs. Diversity in expression of downstream synthases results in the generation of 1 or 2 dominant PGs by individual cells (1). There are 2 isoforms found in most animals; PGHS1, also referred to colloquially as cyclooxygenase 1 (COX1), is generally essential for homeostatic processes, including integrity of gastric mucosa, platelet aggregation, kidney water-salt balance, and normal vascular tone, while PGHS2 (COX2) is induced by various inflammatory stimuli (2). The primary mechanism of action of traditional NSAIDs is inhibition of PGHS, which results in antithrombotic and antiinflammatory efficacy, as well as adverse effects involving the gastrointestinal tract and reproductive system (1–4). NSAIDs selective for inhibition of PGHS2 retain antiinflammatory efficacy. However, as PGHS2 is not expressed in platelets, they do not inhibit platelet function. Indeed, they may predispose to myocardial infarction and stroke via suppression of the endogenous inhibitor of platelet aggregation, prostacyclin (PGI_2) (5).

PGs are involved in luteolysis, implantation, and parturition in reproductive tissues (6). Previous studies demonstrated that in mice lacking cytosolic phospholipase A_2 (7) or the $PGF_{2\alpha}$ receptor (FP) (8), parturition is disturbed critically. Likewise, in PGHS1-null mice, onset of parturition is delayed, which leads to high neonatal mortality (9, 10), and this can be rescued by $PGF_{2\alpha}$ replacement (10). Thus, $PGF_{2\alpha}$ from PGHS1 metabolism is required for normal parturition in mice. However, the levels required to support initiation of labor remain unclear.

Low-dose aspirin is effective in the secondary prevention of both heart attack and stroke and in the primary prevention of nonfatal myocardial infarction (11). Although many mechanisms have been invoked, inhibition of platelet PGHS1-derived thromboxane A_2 (TxA_2) is sufficient to explain the cardioprotective benefits from low-dose aspirin that have been detected in randomized controlled clinical trials (12). Biosynthesis of TxA_2 is increased in preeclampsia, and it relates to the severity of the disease (13). There is some controversy as to whether low-dose aspirin, which preferentially targets PGHS1, may prevent preeclampsia or ameliorate its complications (14–17). Furthermore, low-dose aspirin differs among tissues in its impact on PGHS1-derived eicosanoids. While inhibition of platelet-derived TxA_2 is virtually complete, inhibition of PG production by nucleated cells, while substantial, is less pronounced, due to resynthesis of PGHS1 (18). The consequences of such differential inhibition of PG formation are poorly understood. For example, the antiinflammatory properties of low-dose aspirin remain controversial, and the mechanism of its impact on the gastrointestinal tract is poorly understood. In the case of preeclampsia, a coincidental impact by low-dose aspirin on parturition would confound interpretation of the efficacy of platelet inhibition. To address these issues, we created a mouse with hypomorphic PGHS1 alleles, designated $PGHS1^{Neo/Neo}$, in which substantial but incomplete suppression of PGHS1-derived eicosanoids achieved by low-dose aspirin therapy in humans is mimicked (18).

Nonstandard abbreviations used: AA, arachidonic acid; ASA/WT, low-dose aspirin–treated WT; COX1, cyclooxygenase 1; LC/MS/MS, liquid chromatography/mass spectrometry/mass spectrometry; Neo cassette, neomycin resistance cassette; OT, oxytocin; OTR, OT receptor; PGHS, PGH synthase; PPP, platelet-poor plasma; PRP, platelet-rich plasma; TPA, tetradecanoyl phorbol acetate; TxA_2, thromboxane A_2.

Conflict of interest: The authors have declared that no conflict of interest exists.

Citation for this article: *J. Clin. Invest.* **115**:986–995 (2005). doi:10.1172/JCI200523683.

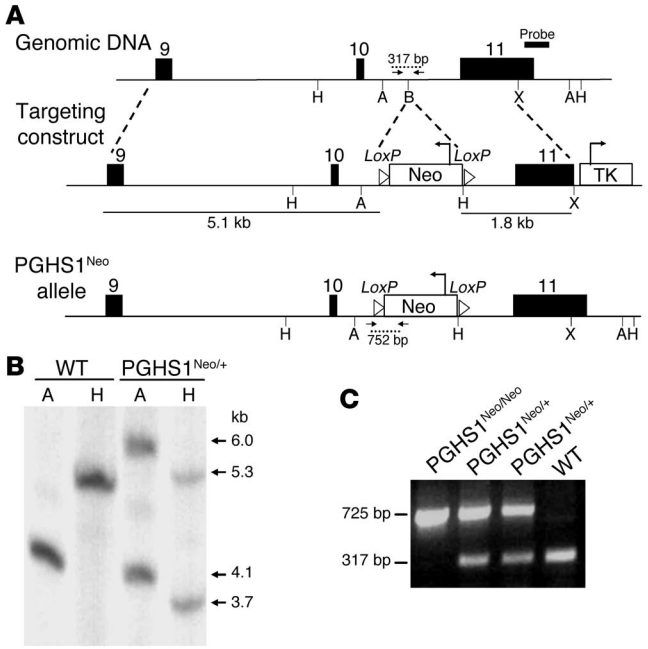

Figure 1
Generation of PGHS1^{Neo} mice. (**A**) Targeting strategy. Numbers indicate known coding exons. Dashed lines indicate regions for homologous recombination; dotted lines represent fragments generated by PCR genotyping. TK, thymidine kinase. Restriction sites: A, *Apa*LI; B, *Bam*HI; H, *Hind*III; X, *Xba*I. (**B**) Identification of PGHS1^{Neo} allele by Southern blot analysis. The 4.1- and 6.0-kb bands represent WT and targeted alleles, respectively, when *Apa*LI was used for DNA digestion, while the 5.3- and 3.7-kb bands represent the corresponding alleles with *Hind*III digestion. (**C**) PCR genotyping of tail biopsies from WT (317 bp) and PGHS1^{Neo} (752 bp) mice.

Results

Generation of PGHS1^{Neo} hypomorphic allele mice. We inserted a neomycin resistance cassette (Neo cassette) into the middle of intron 10 of the PGHS1 gene by targeting ES cells (Figure 1A). Insertion of this cassette within intronic sequences has been reported previously to generate a hypomorphic allele or knockdown of gene expression to very low levels (19–21). Following homologous recombination and positive/negative double selection, resistant clones were screened by Southern blot analysis. Only 1 of 1,152 G418-ganciclovir–resistant clones underwent homologous recombination (Figure 1B). PGHS1$^{Neo/+}$ ES cells were used to generate chimeras, which yielded germline transmission of the PGHS1^{Neo} allele. A PCR-based genotyping assay was developed based on detection of the loxP sites surrounding the Neo cassette in intron 10 (Figure 1C).

Characterization of PGHS1^{Neo} mice. PGHS1 protein expression in nonstimulated peritoneal macrophages from PGHS1$^{Neo/Neo}$, PGHS1$^{Neo/+}$, and PGHS1$^{+/+}$ (WT) mice was examined by Western blot analysis. This analysis revealed that PGHS1 was dramatically reduced in PGHS1$^{Neo/Neo}$ unstimulated PGHS1$^{Neo/Neo}$ macrophages (Figure 2A) to approximately 10% of WT levels (Figure 2, A and B). LPS-induced PGHS2 expression (Figure 2, A and C) was comparable among WT, PGHS1$^{Neo/Neo}$, and PGHS1-null macrophages, which indicated no compensatory gene expression alterations as a result of PGHS1 knockdown. We analyzed peritoneal macrophages for PGE_2 biosynthesis with exogenous AA as substrate to determine the effect of the hypomorphic PGHS1 allele on PG biosynthesis. PGE_2 production was reduced by 75% in PGHS1$^{Neo/Neo}$ cells compared with WT (Figure 2D). Under these conditions, without stimulation, PGHS2 is undetectable in macrophages and contributes little to PGE_2 synthesis. We also examined the expression of PGHS1 in other tissues (stomach, kidney) where PGHS1 is constitutively expressed in normal mice using quantitative RT-PCR and found that the suppression was similar (70–73%) (Figure 2E). Taken together, these results indicate that PGHS1$^{Neo/Neo}$ mice are globally hypomorphic for PGHS1 expression.

Ear inflammation in response to AA and capsaicin is reduced in PGHS1$^{Neo/Neo}$ mice. Since the role of PGHS1 and low-dose aspirin in inflammation remains controversial, we determined whether hypomorphic PGHS1 mice had an altered inflammatory response by examining the effects of evoked ear swelling (22, 23). Ear inflammation was induced by topical application of AA, phorbol ester tetradecanoyl phorbol acetate (TPA), croton oil, or capsaicin in 3 groups of mice. PGHS1-KO mice exhibited a significantly reduced inflammatory response to AA, measured as an increase in ear weight ($P < 0.05$), as previously reported (9), and PGHS1$^{Neo/Neo}$ mice showed a similar response (PGHS1-KO, 6.5 ± 1.5 mg, $n = 7$; PGHS1$^{Neo/Neo}$, 7.6 ± 1.0 mg, $n = 7$); inflammation was markedly reduced compared with WT littermates (11.3 ± 1.2 mg, $n = 8$; $P < 0.05$) (Figure 3A). Similarly, both PGHS1$^{Neo/Neo}$ and PGHS1-KO mice displayed significant inflammatory protection in response to capsaicin compared with WT (55–60% vs. WT) (Figure 3C). In contrast, TPA-induced (Figure 3B) and croton oil–induced (data not shown) inflammation did not differ among the 3 groups of mice.

Carrageenan-induced paw edema is diminished in PGHS1$^{Neo/Neo}$ mice. Carrageenan-induced paw edema mediated by local PGs, histamine, and 5-hydroxytryptamine represents a classical model of edema formation and hyperalgesia, which has been extensively exploited in the development of NSAIDs (23). Edema, measured as increased paw thickness (Figure 3D), was significantly less in PGHS1$^{Neo/Neo}$ and PGHS1-KO mice than in WT controls in the absence or presence of treatment with the PGHS2 selective inhibitor celecoxib (PGHS1$^{Neo/Neo}$: 49% and 58% decrease, respectively; PGHS1-KO: 57% and 54% decrease, respectively.)

Platelet function is diminished in PGHS1$^{Neo/Neo}$ mice. PGHS1, but not PGHS2, is highly expressed in mature human platelets (24) and is the dominant source of TxA_2 biosynthesis under physiological conditions in humans (25). Pharmacological studies suggest that inhibition of the capacity of human platelets to generate TxA_2 by more than 95% is necessary to accomplish inhibition of TxA_2-dependent platelet aggregation ex vivo (26), while provision of as little as 10% normal platelets is sufficient to restore function after exposure to aspirin in vitro (27).

We isolated platelet-rich plasma (PRP) from PGHS1$^{Neo/Neo}$ and WT littermates and PGHS1-KO mice to investigate the platelet aggregation response to AA ex vivo (Figure 4A). The platelets from PGHS1$^{Neo/Neo}$, PGHS1-KO, and low-dose aspirin–treated WT mice (ASA/WT) failed to aggregate in response to concentrations of AA that were effective in WT platelets. Plasma TxB_2 was depressed 97% in PGHS1$^{Neo/Neo}$ mice (280 ± 10 pg/ml) (Supplemental Table 1; supplemental material available online with this article; doi:10.1172/JCI200523683DS1) compared with WT littermates (8,610 ± 50 pg/ml), which is similar to the inhibition achieved by low-dose aspirin in mice (96%) and agrees with the level of inhibition in humans (18,

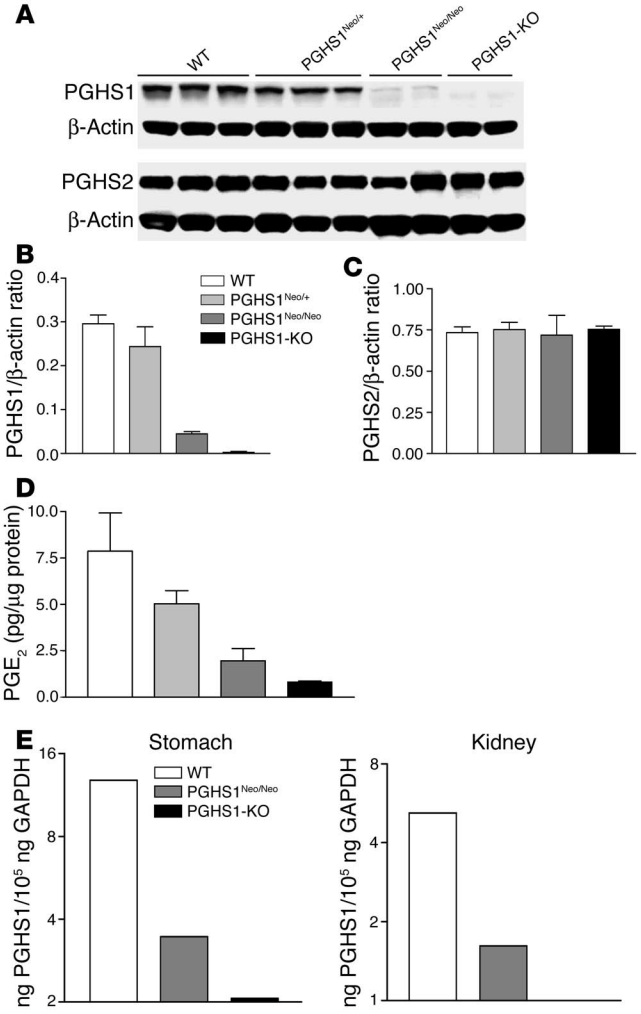

Figure 2
PGHS1 is downregulated in PGHS1$^{Neo/Neo}$ mice. (**A**) Western blot analysis of PGHS1 in nonstimulated (top panel) and PGHS2 in LPS-stimulated (bottom panel) peritoneal macrophages. PGHS1 and PGHS2 protein expression in nonstimulated (**B**) and LPS-stimulated (**C**) macrophages, respectively. (**D**) PGE_2 production by nonstimulated peritoneal macrophages from PGHS1$^{Neo/Neo}$ mice (4 mice/group; repeated 3 times). (**E**) Real-time RT-PCR for determination of PGHS1 mRNA levels in stomach and kidney tissue of PGHS1$^{Neo/Neo}$, WT, and PGHS1-KO mice (n = 8).

25, 26). Plasma TxB_2 in PGHS1-KO mice (120 ± 10 pg/ml) was even lower. A residual 2–3% of WT platelet capacity to generate TxB_2 was retained in platelets from PGHS1$^{Neo/Neo}$ mice (Supplemental Table 1), while even less TxB_2 formation was observed in the PGHS1-KO group (0.1–0.3% of the WT level). To further confirm decreased platelet function in PGHS1$^{Neo/Neo}$ mice, we performed bleeding time assays. Compared with that in normal WT littermates (1.9 ± 0.3 min, n = 15; P < 0.001), tail bleeding time was significantly prolonged in PGHS1$^{Neo/Neo}$ (8.6 ± 2.1 min, n = 12) and PGHS1-KO (12.6 ± 2.1 min, n = 11) mice (Figure 4B), although the 2 latter groups did not differ significantly from each other.

Protection against thrombosis in vivo in PGHS1$^{Neo/Neo}$ mice. Since platelets from both PGHS1$^{Neo/Neo}$ and PGHS1-KO mice have defective generation of thromboxane and impaired aggregation responses ex vivo, we determined their response to thrombotic stimuli in vivo (28, 29). Both PGHS1$^{Neo/Neo}$ and PGHS1-KO mice were resistant to AA-induced thrombosis in vivo (Figure 5A), while nearly all WT mice died at both the AA doses — 50 mg/kg and 100 mg/kg — that we tested. Moreover, in a model of arterial photochemical injury, latency time to arterial occlusion by clot formation as measured by Doppler flow was significantly increased in PGHS1$^{Neo/Neo}$ (67.8 ± 10.8 min) and PGHS1-KO (75.5 ± 13.1 min) mice compared with WT controls (39.4 ± 4.7 min) (Figure 5, B and C).

Hypomorphic expression of PGHS1 or low-dose aspirin treatment does not affect initiation of full-term labor in mice. PGHS1-KO mice are fertile but have delayed onset of parturition, as described previously (9, 10). To examine the role of hypomorphic PGHS1 expression in the initiation of labor in mice, we established timed matings of males and females of PGHS1$^{Neo/Neo}$, PGHS1$^{Neo/+}$, PGHS1-KO, WT, and ASA/WT genotypes. The average gestational length for PGHS1$^{Neo/Neo}$ mice was 19.6 days (Table 1), which did not differ significantly from that of PGHS1$^{Neo/+}$ (19.7 ± 0.2 d), WT (19.5 ± 0.2 d), and ASA/WT (19.3 ± 0.1 d) mice. Parturition was significantly delayed in PGHS1-KO mice (21.1 ± 0.3 d; P < 0.01), which resulted in 46% of newborn pups dying within the first 24 hours after birth. The litter size and development of PGHS1$^{Neo/Neo}$, PGHS1$^{Neo/+}$, and WT mice were similar (Table 1). Moreover, the normal parturition of PGHS1$^{Neo/Neo}$ mice was delayed by the selective PGHS1 inhibitor SC-560 (21.5 ± 0.5 d; Supplemental Table 2), which is consistent with studies described in WT mice (3).

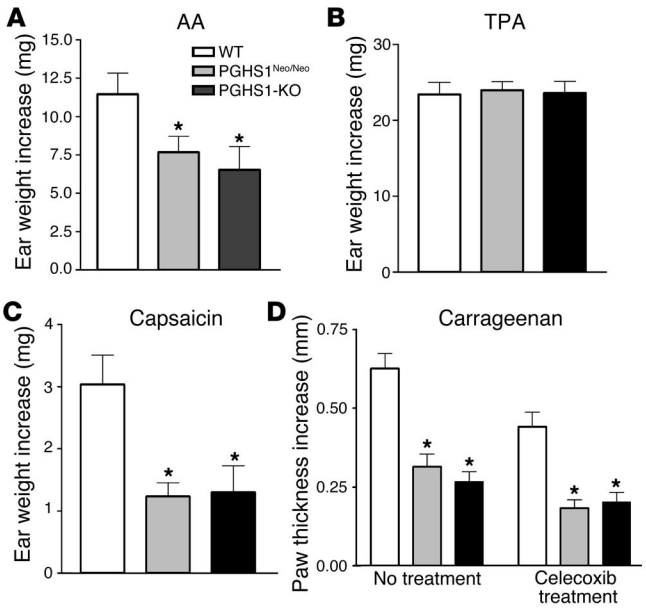

Figure 3
Induction and evaluation of inflammatory response of PGHS1$^{Neo/Neo}$ mice. Data are expressed as ear weight increase of an 8-mm diameter biopsy after AA (**A**), TPA (**B**), or capsaicin (**C**) treatment (left ear) compared with vehicle treatment (right ear). *P < 0.05 versus WT (n = 6–12). (**D**) Carrageenan-induced paw edema. Results are displayed as increase in paw thickness. For the celecoxib treatment group, 8 week old mice were fed diet containing 800 parts per million celecoxib for 4 weeks. *P < 0.05 versus WT (n = 6–9).

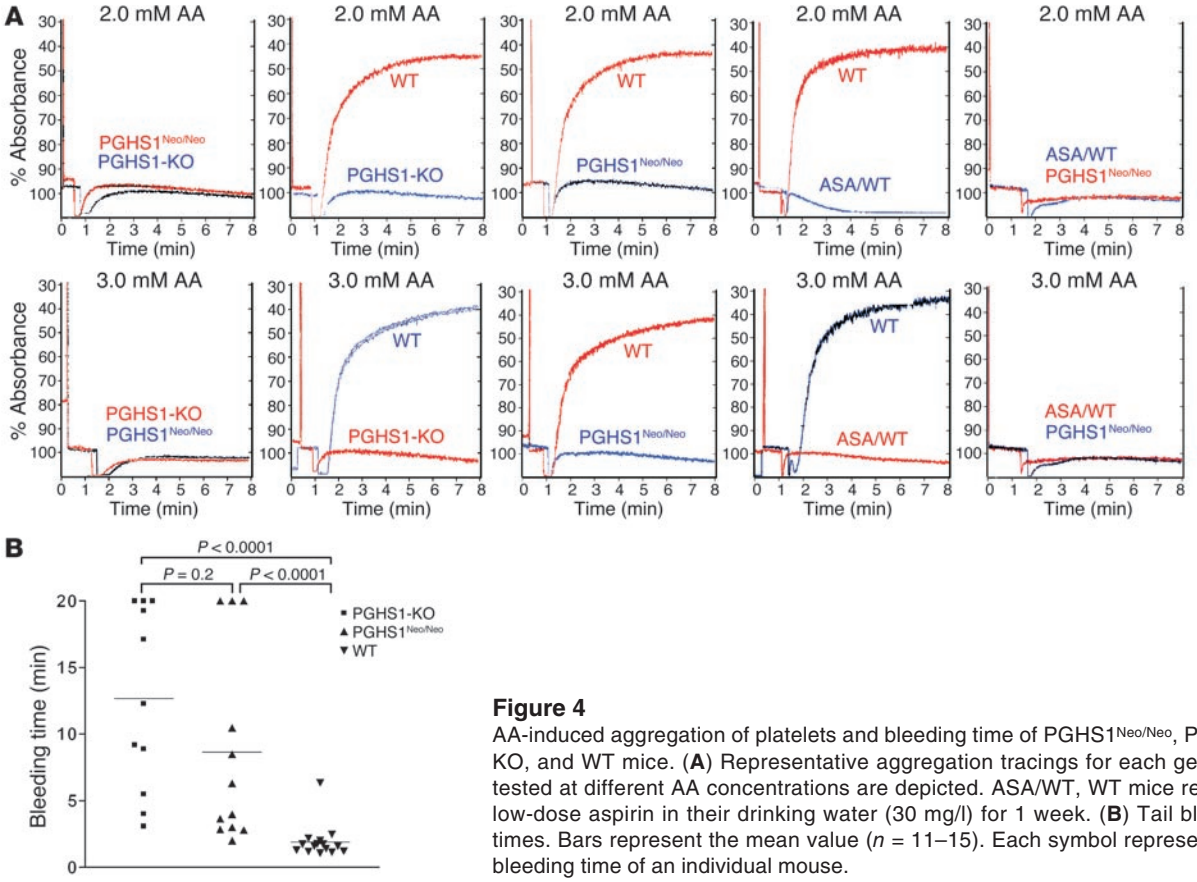

Figure 4
AA-induced aggregation of platelets and bleeding time of PGHS1$^{Neo/Neo}$, PGHS1-KO, and WT mice. (**A**) Representative aggregation tracings for each genotype tested at different AA concentrations are depicted. ASA/WT, WT mice received low-dose aspirin in their drinking water (30 mg/l) for 1 week. (**B**) Tail bleeding times. Bars represent the mean value (n = 11–15). Each symbol represents the bleeding time of an individual mouse.

PGHS1 expression is upregulated in the uterus during late gestation (d 16.5) and decreases to undetectable levels after delivery (10, 30), which is consistent with its requirement for normal initiation of parturition in the mouse. We analyzed PGHS1 protein (at d 18.5) and mRNA (at d 17.5) levels in uterus of PGHS1$^{Neo/Neo}$ mice compared with WT and PGHS1-KO mice to assess the relative impact of substantial versus complete inhibition of PGHS1-derived eicosanoids. Immunoactivity of PGHS1 was detected in both the cytoplasm and the nucleus, consistent with the known subcellular localization of the enzyme (Figure 6A). Expression was particularly pronounced in the decidua (uterine endometrium of pregnancy) of WT mice but was weakly expressed in PGHS1$^{Neo/Neo}$ mice and was absent in deciduas from PGHS1-KO mice. PGHS1 mRNA in PGHS1$^{Neo/Neo}$ mice was 12% of that in WT at day 17.5 of gestation, while mRNA was absent in PGHS1-KO mice (Figure 6B).

Exogenous $PGF_{2\alpha}$ induces a decline in serum progesterone and initiates parturition in many species (31). Moreover, $PGF_{2\alpha}$ administration can rescue the parturition defect in PGHS1-KO mice (10). We measured PG profiles in uterus to characterize further the apparently normal delivery process in hypomorphic PGHS1 mice. Only a small residual capacity to generate uterine PGs was apparent in PGHS1$^{Neo/Neo}$ mice ($PGF_{2\alpha}$, 8%; PGE_2, 3.3%; PGD_2, 3.2% of WT levels) (Figure 6C). However, these levels were sufficient to prepare for the normal onset of labor at day 19 of gestation. By contrast, the residual synthetic capacity in PGHS1-KO mice ($PGF_{2\alpha}$, 1.1%; PGE_2, 1.1%; PGD_2, 0.4% of WT levels) was insufficient to initiate normal parturition at term. Taken together, these findings suggest that the substantial but incomplete depression of extraplatelet PG formation by treatment with low-dose aspirin would be insufficient to delay initiation of parturition.

Alterations of hormones and oxytocin receptor in PGHS1$^{Neo/Neo}$ mice during pregnancy. Mice lacking the FP exhibit parturition failure due to impaired withdrawal of serum progesterone at term, which indicates an interaction of the ligand with ovarian receptors to induce luteolysis and initiate parturition (8). We determined the serum progesterone and estradiol levels in PGHS1$^{Neo/Neo}$ mice during late-stage pregnancy. Mice of each genotype demonstrated high plasma progesterone levels at day 16.5 of pregnancy (Figure 7A), indicative of sustained activity of the corpus luteum. Just prior to delivery, at day 19, the progesterone levels in PGHS1$^{Neo/Neo}$ mice decreased markedly (≈80%), as did those in WT mice. However, PGHS1-KO mice maintained high progesterone levels, which resulted in delayed onset of parturition. As expected, estradiol levels did not differ among the genotypes, as the placenta becomes their main source during pregnancy (Figure 7B). Thus, PGHS1$^{Neo/Neo}$ mice appear to maintain normal sex hormone status during pregnancy.

Oxytocin (OT) is one of the most potent uterotonins, and OT receptors (OTRs) are markedly induced in the myometrium during late gestation in all mammalian species (32–36). We analyzed the mRNA levels in pregnant PGHS1$^{Neo/Neo}$, PGHS1 KO, and WT mice using semiquantitative RT-PCR to investigate the regulation of OTR mRNA expression in uterus at day 19 of gestation. OTR mRNA increased in abundance at term in both PGHS1$^{Neo/Neo}$ and WT mice (Figure 7, C and D), in contrast to PGHS1-KO mice, in which OTR mRNA levels were barely detectable. Interestingly, OTR mRNA expression in PGHS1$^{Neo/Neo}$ mice was even higher (50%) than

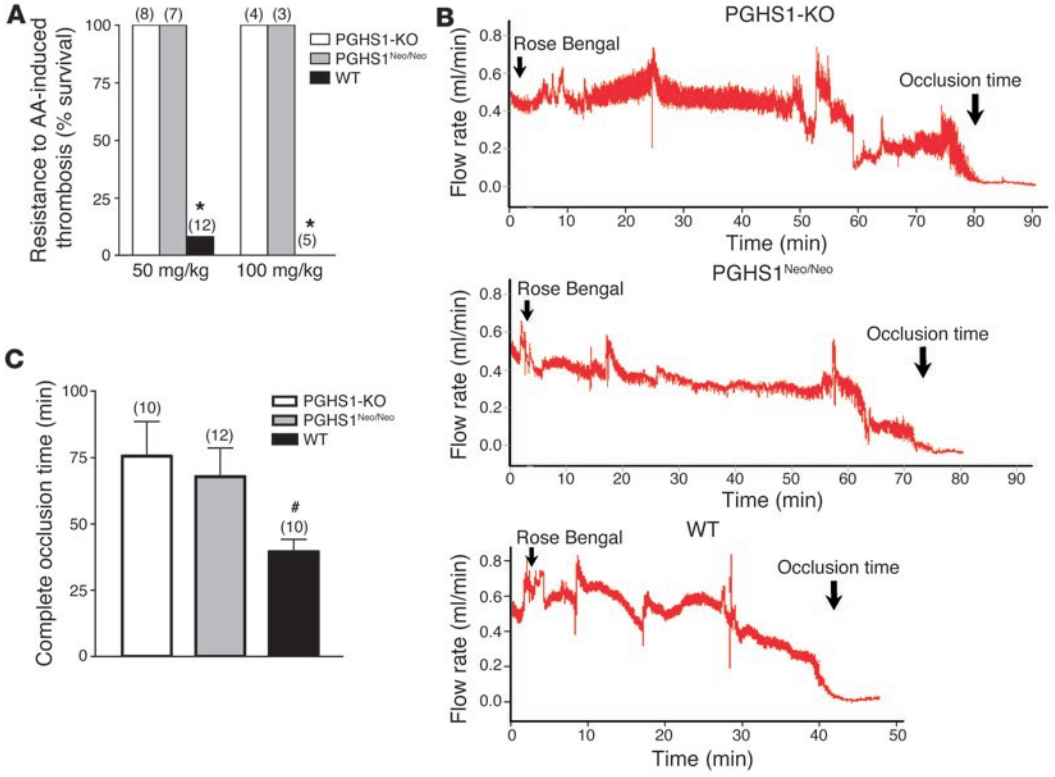

Figure 5

Protective effect against AA- and photochemical-induced thrombosis in hypomorphic PGHS1 mice. Mice were injected with AA via the tail vein (**A**) or with Rose Bengal via the jugular vein, followed by laser excitation at the right carotid artery (**B** and **C**). Percent survival of each group in **A** is indicated (*$P < 0.001$, as determined by Fisher's exact test). (**B**) Representative Doppler flow tracings after photochemical injury in PGHS1-KO (top panel), PGHS1$^{Neo/Neo}$ (middle panel), and WT (bottom panel) mice. Rose Bengal injection and clot occlusion times are marked with arrows. (**C**) Combined data for photochemical-induced arterial injury model. The number of mice examined is indicated in parentheses. #$P < 0.05$ vs. PGHS1-KO and PGHS1$^{Neo/Neo}$ mice.

in WT mice (Figure 7D). The results suggest that regulation of OTR expression in PGHS1$^{Neo/Neo}$ mice is near normal during pregnancy.

Ovarian morphology of PGHS1$^{Neo/Neo}$ mice. During pregnancy, the corpus luteum, from formation to regression, is accompanied by tissue remodeling, physiological angiogenesis, and tissue degradation (36, 37). $PGF_{2\alpha}$ is considered to be an important endogenous luteolytic mediator (31, 38, 39), so we assessed ovarian properties of PGHS1$^{Neo/Neo}$, PGHS1-KO, and WT mice during pregnancy. The size and weight of ovaries from PGHS1-KO mice (11.22 ± 0.95 mg, $n = 5$) at late gestation (day 19) were significantly greater than those of ovaries from WT (7.60 ± 0.77 mg, $n = 5$; $P < 0.01$) and PGHS1$^{Neo/Neo}$ (8.08 ± 0.83 mg, $n = 6$; $P < 0.05$) mice (Figure 8, A and B), which implies that the luteal regression phase in PGHS1-KO mice was delayed compared with that in both PGHS1$^{Neo/Neo}$ and WT mice. No overt differences were observed between WT and PGHS1$^{Neo/Neo}$ mice ($P = 0.70$). Moreover, no significant differences in ovarian weights of adult nongravid females were observed among the 3 different genotypes, which further supports the concept that the elevated ovarian weights of PGHS1-KO mice at late gestation result from delayed luteal regression, consistent with plasma progesterone alterations in PGHS1-KO mice (Figure 7A).

During late gestation, ovarian $PGF_{2\alpha}$ production in PGHS1$^{Neo/Neo}$ mice was reduced by 84% (10.4 pg/mg ovary) as compared with WT (64.2 pg/mg ovary), while $PGF_{2\alpha}$ levels were very low in PGHS1-KO ovaries (1.3 pg/mg ovary) (Figure 8C). A similar pattern of $PGF_{2\alpha}$ production was observed in nongravid ovaries. These data are consistent with a residual of approximately 15% of normal ovarian $PGF_{2\alpha}$ production from PGHS1 being sufficient to promote timely luteolysis for initiation of labor at late gestation. The contribution of PGHS2 to $PGF_{2\alpha}$ production in this setting is negligible.

Cre-mediated deletion of the Neo cassette restores PGHS1 expression level. The Cre recombinase–loxP (Cre/loxP) system is a powerful tool to modify genes in a cell- and stage-specific manner (40), and EIIa Cre transgenic mice, expressing Cre recombinase at the early embryo stage (41), are a common model for generating conditional KOs (42). We crossed PGHS1$^{Neo/Neo}$ mice with EIIa Cre transgenic mice, and the removal of the Neo cassette was detected by PCR (Supplemental Figure 1A), and designated the offspring PGHS1$^{loxp/loxp}$ mice. Using Western blot analysis with peritoneal macrophage protein, we found that the expression level of Cre-deleted PGHS1$^{loxp/loxp}$ mice was comparable to that of WT mice (Supplemental Figure 1B). This inducible gene repair was further supported by measurements of PGE_2 derived from PGHS1 (Supplemental Figure 1C).

Discussion

We have provided new insights into eicosanoid signaling using what we believe to be a novel mouse model of partially disrupted PGHS1 function. The impact of low-dose aspirin is mimicked in our model, in that near complete inhibition of PGHS1-derived

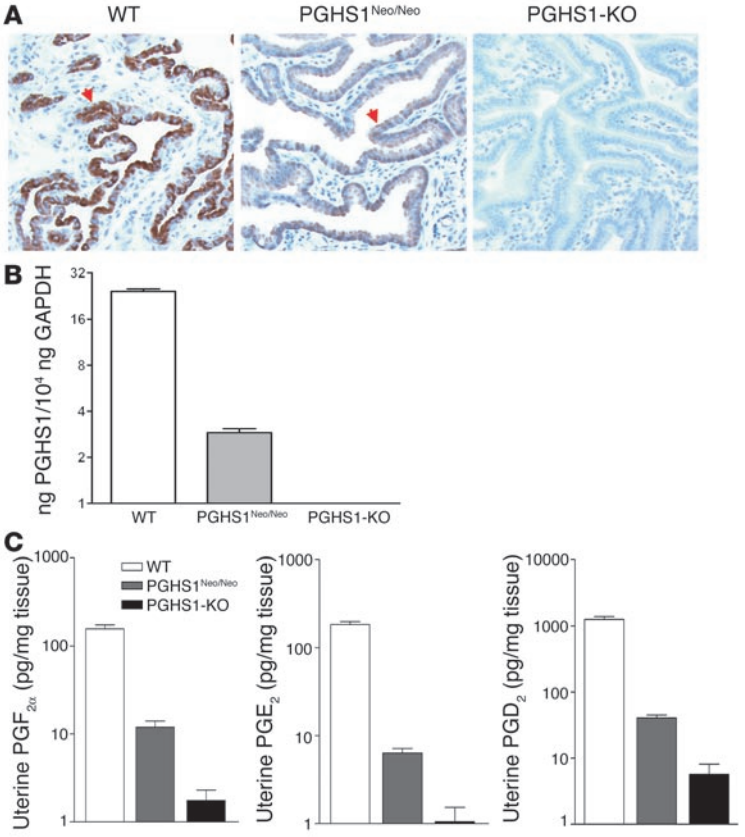

Figure 6
PGHS1 expression and PG profiles in uterus during late-stage pregnancy. (**A**) Immunohistochemical analysis of PGHS1 in uterus at gestation day 18.5 (magnification, ×200). Red arrows represent PGHS1 staining within decidua (endometrium). (**B**) PGHS1 gene expression in uterus at gestation day 17.5 by real-time RT-PCR detection. (**C**) PG profiles in PGHS1$^{Neo/Neo}$, PGHS1-KO, and WT mice at gestation day 19. PGs were extracted from uteri isolated from each group and measured by LC/MS/MS. $PGF_{2\alpha}$, PGE_2, and PGD_2 levels in PGHS1$^{Neo/Neo}$ mice (n = 6) were 8%, 3.3%, and 3.2%, respectively, of those in WT mice (n = 10).

TxA_2 is achieved in platelets, while substantial but incomplete PG inhibition is achieved in nucleated cells. Thus, while thrombosis is prevented and inflammation attenuated by PGHS1 knockdown, parturition is sustained. These discordant properties have implications for the interpretation and design of studies of low-dose aspirin in preeclampsia, reemphasize the contribution of PGHS1 to inflammation, and reveal that PGHS1 but not PGHS2 sustains normal parturition in mice. Secondly, the ability to alter PGHS1-mediated PG synthesis in an inducible manner will allow further exploration of the interplay of PGHS1 with the inducible PGHS2 enzyme in vivo.

Parturition is considered a complex event, consisting of many biochemical and physiological steps with associated signaling molecules. During parturition, labor can be separated into 2 phases after uterine quiescence (43). Progesterone plays an essential role in the preparation for and maintenance of pregnancy and is elevated during quiescence. Just before onset of labor, the uterus and ovaries are coordinately regulated to prepare for labor, and uterine PGHS1 is progressively induced in late pregnancy (10, 30), which results in an increase of $PGF_{2\alpha}$. In our hypomorphic PGHS1 mouse model, only 8% of normal $PGF_{2\alpha}$ levels are sufficient to lead to strong diminution of serum progesterone levels and the consequent upregulation of OTR expression. Surprisingly, OTR expression appears to be even greater in the hypomorphic PGHS1$^{Neo/Neo}$ female mice (in which $PGF_{2\alpha}$ levels are lower but OTR levels are higher) at late gestation, perhaps as a compensatory mechanism in vivo whereby the signaling components are reprogrammed to new set points vis-à-vis WT controls to coordinate uterine contraction at term. $PGF_{2\alpha}$ derived from PGHS1 induction in the ovary (10) triggers onset of labor, which is essential for luteolysis and the decline in serum progesterone (8, 43). Thus, minimal PGHS1 expression is sufficient for these physiological procedures to initiate term parturition. Only after initiation of labor does induction of PGHS2 (29, 44, 45) and OT-OTR interaction contribute to the active phase of parturition.

The relationship between inhibition of TxA_2 generation by platelets and TxA_2-dependent platelet aggregation is strikingly nonlinear (26). Indeed, this nonlinear relationship explains the inability of traditional NSAIDs to afford cardioprotection. Inhibition of platelet function wears off more rapidly than inhibition of platelet thromboxane generation, consistent with the nonlinear relationship between these variables (46). Studies in humans suggest that inhibition of platelet PGHS1 attains functional relevance when the capacity to generate TxA_2 is reduced by 95%. Here we show that inhibition of capacity by 97–98 % in the hypomorphic mice is sufficient to prevent induction of thrombosis and attenuate arterial clot occlusion in vivo in 2 distinct models. Thus, the impact of chronic therapy with low-dose aspirin is likely mimicked in these mice. It has been suggested, although controversially, that PGHS1 may con-

Table 1
Normal parturition in PGHS1$^{Neo/Neo}$ and low-dose aspirin–treated mice but not in PGHS1-KO mice.

Maternal genotype	Paternal genotype	No.	Labor onset, d (range)	Avg. litter	Survival for 24 h (%)
PGHS1$^{Neo/Neo}$	PGHS1$^{Neo/Neo}$	8	19.6 ± 0.2 (19.0–20.5)	7.3 ± 1.1	90.0
PGHS1$^{Neo/+}$	PGHS1$^{Neo/Neo}$	7	19.7 ± 0.2 (19.5–20.5)	7.3 ± 1.2	88.6
ASA/WT[A]	WT	6	19.3 ± 0.1 (18.0–19.5)	8.4 ± 1.6	92.3
PGHS1-KO	PGHS1-KO	10	21.1 ± 0.3[B] (20.0–22.5)	8.7 ± 0.7	54.0[C]
WT	WT	7	19.5 ± 0.2 (19.0–20.0)	6.8 ± 0.5	89.5

[A]WT mice received low-dose aspirin in their drinking water (30 mg/l) starting on gestation day 7. [B]$P < 0.001$ vs. PGHS1$^{Neo/Neo}$, PGHS1$^{Neo/+}$, ASA/WT, and WT mating. [C]$P < 0.05$ vs. PGHS1$^{Neo/Neo}$, PGHS1$^{Neo/+}$, ASA/WT, and WT mating. Avg., average.

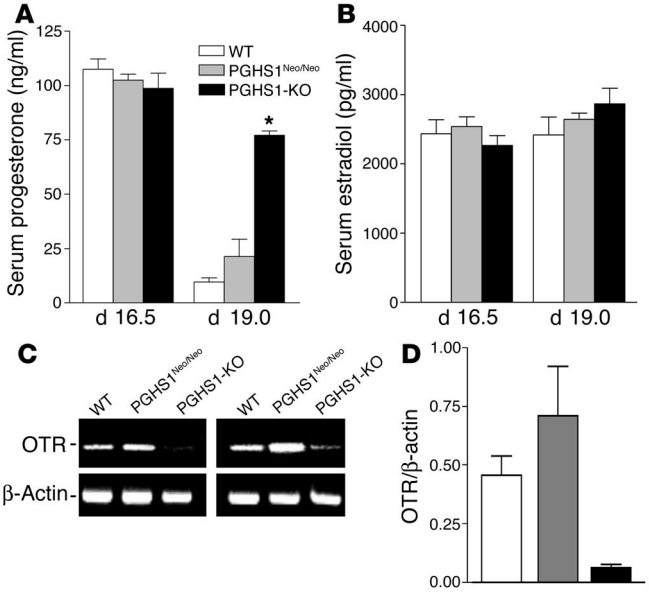

Figure 7
Serum sex hormones and uterine OTR expression in PGHS1$^{Neo/Neo}$, PGHS1-KO, and WT mice at late gestation. (**A** and **B**) Serum progesterone and estradiol concentrations during late gestation, respectively. Blood was collected via the saphenous vein from mice of each genotype group (n = 4–10) and concentration was determined by sequential competitive immunoassay. *P < 0.001 versus PGHS1$^{Neo/Neo}$ and WT mice at day 19. (**C**) mRNA expression of OTR in uterus at gestation day 19. Semiquantitative RT-PCR was performed with primers spanning one 11-kb intron to avoid genomic DNA contamination. (**D**) Relative level of OTR to β-actin expression.

tribute to PG synthesis in inflammation (47). Indeed, both PGHS1 and PGHS2 are coexpressed in human atherosclerotic lesions (48), and low doses of aspirin may exhibit antiinflammatory properties in atherosclerosis-prone mice (49). A role for inhibition of PGHS1-derived PGs by low-dose aspirin treatment in inflammation would accord with our present findings.

The PGHS1$^{Neo/Neo}$ model may prove a useful genetic approach to probing the therapeutic potential of low-dose aspirin in such unconventional settings. A further example is in the use of low-dose aspirin in the prevention and treatment of preeclampsia. Here the utility of such a therapeutic intervention remains controversial. One concern has been that PGHS1 inhibition might negatively affect parturition, thus confounding the potential benefit. Here, we show quite clearly in the PGHS1-knockdown mice that inhibition of platelet activation in vivo can be attained while retaining reproductive integrity. Thus, our findings indicate the feasibility of using low-dose aspirin or selective inhibitors of PGHS1 to prevent platelet activation in pregnant females without affecting their capacity for normal delivery. Finally, aside from the implications of this finding for the design of studies of aspirin in preeclampsia, our knockdown mice can be utilized to probe the role of TxA_2 in models of preeclampsia and intrauterine growth retardation (50).

Emerging evidence has implicated PGHS1, in addition to PGHS2, in skin and intestinal tumorigenesis (51–53), as well as in the inflammatory processes. Moreover, NSAIDs exert protective effects in several neurodegenerative disorders including Alzheimer and Parkinson diseases (54). Removal of the Neo cassette in our PGHS1-knockdown mice by Cre-mediated recombination restores normal expression of PGHS1. Thus, this model provides an opportunity to clarify the role of PGHS1 in various disease models by crossing to inducible- or lineage/tissue–specific Cre transgenic mice.

In summary, we have developed a mouse model with reduced PGHS1 expression by gene targeting. We demonstrate that variable but trivial residual capacity to generate eicosanoids, as might be attained with low-dose aspirin treatment, is compatible with inhibition of both inflammation and thrombosis in vivo. The ability to modulate PGHS1 global expression reversibly in mice will allow us further to decipher the role of this isozyme in the pathogenesis of disease.

Methods

Creation of PGHS1^{Neo} mice. To construct the PGHS1^{Neo} targeting vector, we amplified a 5.1-kb *Bam*HI restriction fragment containing the ninth and tenth exons and adjacent intervening sequences of PGHS1 from 129S6/SvEvTac mouse genomic DNA using the Expand Long Template PCR System (Roche Diagnostics Corp.) with primers *Bam*HI forward (5′-TTGGATCCGTCATTGAGGAGTATGTGCAGCAC-3′) and reverse (5′-TTGGATCCCCTTAAGTGGAATAAAGG-3′) and ligated downstream of the floxed PGK-Neo^r gene cassette at the *Xho*I site in a modified pPNT vector (55) with blunt ends. A 1.8-kb *Xba*I restriction fragment including partial eleventh exon of PGHS1 was amplified with primers *Xba*I forward

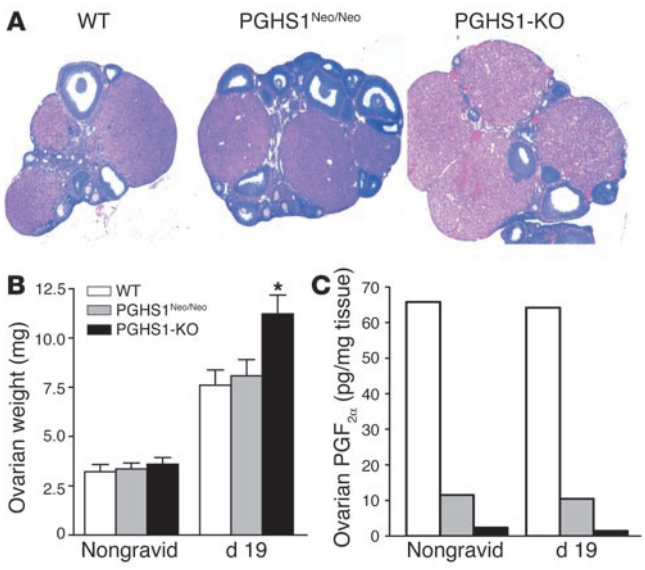

Figure 8
Corpus luteum histology and ovarian $PGF_{2\alpha}$ levels at day 19 of gestation in WT, PGHS1$^{Neo/Neo}$, and PGHS1-KO mice. (**A**) Representative light photomicrographs (magnification, ×40) of ovarian sections from WT, PGHS1$^{Neo/Neo}$, and PGHS1-KO females at gestation day 19. (**B**) Ovarian weights from nongravid females and pregnant mice at gestation day 19. Weights from both ovaries of each mouse were measured. n = 3–6; *P < 0.05 versus PGHS1$^{Neo/Neo}$ and WT mice at day 19 of gestation. (**C**) Ovarian $PGF_{2\alpha}$ levels from nongravid females and pregnant mice at gestation day 19. Frozen ovaries from different groups were pooled after weighing and subjected to PG extraction prior to LC/MS/MS analysis.

(5′-AATCTAGATTCTTGTCTGCCACAGGCACATGAC-3′) and reverse (5′-ATGAACCAATTCCACTTCTAGACATTC-3′), then subcloned into the vector at *Xba*I sites upstream of the Neo cassette (Figure 1A). The targeting vector was linearized with *Not*I and introduced by electroporation into TL-1 embryonic stem (ES) cells (kindly provided by P. Labosky, University of Pennsylvania, Philadelphia, Pennsylvania, USA). ES cell culture and DNA transfections were carried out as previously described (56), and the cells were subjected to selection with 250 μg/ml G418 and 2 μM ganciclovir. Homologous recombination events were screened by Southern blot analysis after *Hind*III digestion using a 3′ end probe amplified from genomic DNA with the following primers: forward probe, 5′-AACCCAGTGTCCAGCAAGAATTGCC-3′ and reverse probe, 5′-CCTGGGTCATGTGGTACTGGCATG-3′. Correct targeting events were verified by Southern blot with *Apa*LI digestion of ES cell genomic DNA (Figure 1B). Targeted clones were injected into 3.5-day-postcoital C57BL/6J blastocysts, and resulting chimeras were backcrossed to C57BL/6J to determine germ line transmission of the targeted allele. Subsequent genotyping was performed routinely by PCR on DNA isolated from tail biopsies; primer 1 (5′-TCTGGAGATCGTGACAAGAATCTG-3′), primer 2 (5′-TCTAACTCCACTGTCCAACGTCTG-3′), and primer 1 in Neo cassette (5′-ATCGCCTTCTTGACGAGTTTC-3′) were used for PCR identification. These primers amplified a 317-bp band from the WT allele and a 752-bp band from the targeted allele due to the insertion of Neo cassette (Figure 1C).

Animal breeding and treatments. PGHS1$^{Neo/Neo}$ mice were maintained on a mixed C57BL/6 × 129/Sv genetic background, as were the previously described PGHS1-null mice (9). WT mice were generated from heterozygous PGHS1$^{Neo/+}$ crosses to ensure a similar genetic background. All animals were maintained on a 12-hour light/12-hour dark cycle with normal mouse chow and water provided ad libitum. The morning after pairing was designated as gestation day 0.5 upon detection of a copulation plug. To determine the duration until the onset of labor, we observed pregnant females from the morning of day 18.5 of gestation. The Institutional Animal Care and Use Committee (IACUC) of the University of Pennsylvania approved the experimentation of animals in this study.

To achieve low-dose aspirin conditions, WT littermates (8 weeks old) received aspirin (30 mg/l) in their drinking water as reported previously (49), and inhibition of PGHS1 was assessed by measurement of plasma TxB_2 and ex vivo platelet aggregation induced by stimulation with AA 1 week later. Pregnant females were treated similarly with aspirin from gestation day 7, and time of parturition was monitored, as well as fetal viability until 48 hours after delivery. In some experiments, for PGHS2-selective inhibition, mice were fed ad libitum a normal chow diet containing 800 parts per million celecoxib for 4 weeks.

To eliminate the Neo cassette in vivo from PGHS1^{Neo} mice, EIIa Cre transgenic mice (The Jackson Laboratory) were crossed to PGHS1$^{Neo/Neo}$ mice, and the removal of the Neo gene by site-specific recombination was tested by PCR as described above. A second round of cross-breeding resulted in PGHS^{loxp} mice (see Results).

Isolation of macrophages and assay for PGE_2 release. Mice were sacrificed by CO_2 asphyxiation, and the abdominal skin was sterilized with 70% alcohol. Cold, sterile PBS (5 ml) was injected into the peritoneal cavity as a washing solution. We harvested peritoneal macrophages using a syringe and stored them in an ice bath. Harvested macrophages were washed twice with cold PBS and seeded at 1×10^7 to 2.5×10^7 per 60-mm dish in 3% FBS RPMI 1640 media supplemented with a 1% mixture of penicillin/streptomycin solution. The cells were allowed to adhere for 2 hours, then 1 duplicate was incubated in fresh medium containing 30 μM AA (Cayman Chemical Co.) for 10 minutes, and the medium was collected for PGE_2 assay. Another duplicate was incubated with LPS (5 μg/ml; Sigma-Aldrich) for 16 hours, and cells were collected for immunoblot analysis.

Immunoblot analysis. The procedure for immunoblot has been reported previously (57). In brief, 10 μg protein was loaded to each lane, separated on a 4–10% NuPAGE Bis-Tris gel (Invitrogen Corp.) and transferred to Hybond ECL nitrocellulose membranes (Amersham Biosciences). Goat anti-COX1 polyclonal antibody (Santa Cruz Biotechnology Inc.) at 1:500 dilution, rabbit anti-COX2 polyclonal antiserum (Cayman Chemical Co.) at 1:1,000 dilution, or mouse anti–β-actin monoclonal antibody (Sigma-Aldrich) at 1:5,000 dilution were used as primary antibodies. HRP-conjugated goat anti-mouse IgG (Sigma-Aldrich), HRP-conjugated mouse anti-goat and HRP-conjugated goat anti-rabbit IgG (Sigma-Aldrich), each at 1:10,000 dilution, were used as secondary antibodies, respectively. Signals were detected using ECL (Amersham Biosciences).

PG extraction and analysis. Tissue was weighed when frozen, then homogenized in 100% ethanol for extraction of PGs. Residual tissue was separated by centrifugation, and the supernatant was collected for analysis. The PGs from tissue supernatant or tissue culture were extracted as described previously (58) and then quantitated utilizing liquid chromatography/mass spectrometry/mass spectrometry (LC/MS/MS) analyses (59).

RNA extraction and RT-PCR. Total tissue RNA was extracted with a RNeasy Mini Kit (QIAGEN). Two micrograms of total RNA from different tissues were reverse-transcribed with the TaqMan reverse transcription kit in 100 μl volume (Roche Diagnostics Corp.) The cDNAs were then subjected to semiquantitative RT-PCR and real-time RT-PCR with SYBR Green PCR system (Applied Biosystems). The PCR was performed in 384-well plates with an ABI Prism 7900 Sequence Detection System; data were analyzed with SDS software version 2.0 (Applied Biosystems). The primers were designed by using Primer Express software version 2.0 (Applied Biosystems) and were as follows: mCOX1-1104F, 5′-GTTCCGAGCCCAGTTCCAATA-3′; mCOX-1-1226R, 5′-AACTGCTCGTAGCTGTACTCTTGTGA-3′; mGAPDH-684F, 5′-CATGGCCTTCCGTGTTCCTA-3′; mGAPDH-799R, 5′-ATGCCTGCTTCACCACCTTCT-3′; mOTR-1, 5′-AATCCGCACAGTGAAGATGAC-3′; mOTR-2, 5′-AAGAGCATGGCAATGATGAAG-3′; β-actin-1, 5′-TGGAATCCTGTGGCATCCATG-3′; β-actin-2, 5′-AACGCAGCTCAGTAACAGTCC-3′.

Mouse ear inflammation assays. Capsaicin (40 μg in 10 μl ethanol; Sigma-Aldrich), AA (2 mg in 10 μl acetone), croton oil (0.5 μg in 20 μl acetone; Sigma-Aldrich), or TPA (1 μg in 10 μl acetone; Sigma-Aldrich) was applied to the inside of the left ear, and the same amount of vehicle was applied to the right ear of 8-week-old mice. Ear punches (8 mm) were taken and weighed after 1, 2, 5, or 6 hours treatment, respectively.

Carrageenan-induced paw edema model. Mice (12 weeks old), anesthetized by intraperitoneal injection of 20 mg/kg ketamine hydrochloride, were subjected to subcutaneous injection of 25 μl 1% λ-Carrageenan (Sigma-Aldrich) in 0.9% saline into the plantar region of the left hind paw, while the right paw received the same amount of saline solution. We assessed edema 4 hours later by measuring paw thickness at the metatarsal level using calipers (23).

Platelet aggregation. Blood was isolated from the inferior vena cava of anesthetized mice (80 mg/kg pentobarbital) using a heparinized syringe (15 U/ml blood), then diluted 1:1 with HEPES-Tyrode's buffer and spun at 100 *g* for 7 minutes to remove red cells. Blood from individual mice of each genotype was used for aggregation experiments, with the final platelet count adjusted to 2×10^8/ml with platelet-poor plasma (PPP) from the same mouse. Aggregation was initiated with 5 μl of different concentrations of AA applied to a 250-μl aliquot of PRP and measured in a lumi-aggregometer (Chrono-log Corp.). All experiments were repeated at least 3 times.

Tail-bleeding test. Mice (8–10 weeks old) were anesthetized intraperitoneally with pentobarbital (80 mg/kg), and tails were transected 1 mm from the tip with a sterile scalpel blade. The remaining tail was immersed in 37°C saline, and the time until bleeding stopped for a period of at least 1 minute

was observed and recorded. The experiment was terminated after 20 minutes, after which any mice still bleeding were assigned a value of 20 minutes for the purpose of statistical analysis.

In vivo thrombosis models. Mice (8–10 weeks old) were weighed and anesthetized with pentobarbital (80 mg/kg). In the first model, AA (sodium salt) in PBS at a concentration of 50 or 100 mg/kg was injected via the tail vein. Heart rate was monitored for 15 minutes prior to sacrifice. In the photochemical arterial thrombosis model, Rose Bengal (50 mg/kg; 0.12 ml) in PBS was injected into the jugular vein, and a 1.5-mW green light laser (540 nm) was applied to a defined site of the previously isolated right common carotid artery from a distance of 5 cm for 120 minutes or until thrombosis occurred. A Doppler flow probe connected to a flow meter and computerized data acquisition program was used to monitor flow rate. Mean carotid artery blood flow was monitored for 120 minutes or until stable occlusion occurred, after which the mice still showing blood flow were assigned a value of 120 minutes. Stable occlusion was defined as a blood flow of 0 ml/min for 5 minutes.

Measurement of plasma and AA-activated platelet TxB_2. Mouse blood collected from the inferior vena cava was separated by centrifugation and stored at –70°C as described previously (60) until TxB_2 extraction. Platelets isolated as described above were stimulated with 0.5 to 3 mM AA for TxB_2 production at 37°C for 8 minutes. After centrifugation at 20,500 *g* in an Eppendorf centrifuge for 2 minutes, TxB_2 in the supernatant was determined by LC/MS/MS assay as described (59).

Serum hormone analysis. Serum was prepared from blood collected from the saphenous vein. Estrogen and progesterone levels were determined by sequential competitive immunoassay with IMMULITE Analyzer (Diagnostic Products Corp.) at the clinic laboratory of the Veterinary Hospital of University of Pennsylvania. At least 4 separate groups of pregnant mice were used for hormone measurement.

Ovarian weights and histology. The weights of ovaries from 10-week-old mice at gestation day 19 were determined as described previously (61, 62). After weighing, ovaries were fixed in 10% buffered formalin for 24 hours, processed routinely, and embedded in paraffin for staining with H&E.

PGHS1 immunohistochemistry. Mouse uterine horns fixed in 10% phosphate-buffered formalin were embedded in paraffin and sectioned to evaluate the immunohistochemical localization of PGHS1. After preincubation in goat serum and peroxidase blocking solution, the sections were incubated overnight at 4°C with a rabbit polyclonal anti-mouse PGHS1 antiserum (Cayman Chemical Co.) diluted 1:700. Negative controls were incubated overnight in PBS. After washing with PBS for 10 minutes, the immunohistochemical reaction was accomplished using a commercial avidin-biotin-peroxidase kit (Vectastain Elite; Vector Labs Inc.) with diaminobenzidine as chromogen.

Statistical analysis. Data are presented as mean ± SEM. Analyses were performed by the Student's *t* test, 1-way ANOVA test, or Fisher's exact test (for the data in Figure 5A). $P < 0.05$ was considered as significant. Prism 3.0 software (GraphPad Software) was used for all calculations.

Acknowledgments

We are grateful to Jean Richa and the Transgenic Core Facilities at the University of Pennsylvania for ES cell injection and generation of chimeras. We also thank the clinic laboratory of the Veterinary Hospital, University of Pennsylvania, for assay of mouse serum hormones. We thank Helen Zou and John Lawson for analysis of PGs by LC/MS/MS assay. This work was supported by a grant from the NIH (R01GM063130). C.D. Funk holds a Canada Research Chair in Molecular, Cellular and Physiological Medicine.

Received for publication October 20, 2004, and accepted in revised form February 1, 2005.

Address correspondence to: Colin D. Funk, Departments of Physiology and Biochemistry, Botterell Hall Room 433, Queen's University, Kingston, Ontario K7L 3N6, Canada. Phone: (613) 533-3242; Fax: (613) 533-6880; E-mail: funkc@post.queensu.ca.

Xin-Sheng Chen's present address is: Hematology/Oncology Division, University of Pennsylvania, Philadelphia, Pennsylvania, USA.

1. Smith, W.L., DeWitt, D.L., and Garavito, R.M. 2000. Cyclooxygenases: structural, cellular, and molecular biology. *Annu. Rev. Biochem.* **69**:145–182.
2. Dubois, R.N., et al. 1998. Cyclooxygenase in biology and disease. *FASEB J.* **12**:1063–1073.
3. Loftin, C.D., Trivedi, D.B., and Langenbach, R. 2002. Cyclooxygenase-1-selective inhibition prolongs gestation in mice without adverse effects on the ductus arteriosus. *J. Clin. Invest.* **110**:549–557. doi:10.1172/JCI200214924.
4. Reese, J., et al. 2001. Comparative analysis of pharmacologic and/or genetic disruption of cyclooxygenase-1 and cyclooxygenase-2 function in female reproduction in mice. *Endocrinology.* **142**:3198–3206.
5. FitzGerald, G.A. 2004. Coxibs and cardiovascular disease. *N. Engl. J. Med.* **351**:1709–1711.
6. Goff, A.K. 2004. Steroid hormone modulation of prostaglandin secretion in the ruminant endometrium during the estrous cycle. *Biol. Reprod.* **71**:11–16.
7. Bonventre, J.V., et al. 1997. Reduced fertility and postischaemic brain injury in mice deficient in cytosolic phospholipase A_2. *Nature.* **390**:622–625.
8. Sugimoto, Y., et al. 1997. Failure of parturition in mice lacking the prostaglandin F receptor. *Science.* **277**:681–683.
9. Langenbach, R., et al. 1995. Prostaglandin synthase 1 gene disruption in mice reduces arachidonic acid-induced inflammation and indomethacin-induced gastric ulceration. *Cell.* **83**:483–492.
10. Gross, G.A., et al. 1998. Opposing actions of prostaglandins and oxytocin determine the onset of murine labor. *Proc. Natl. Acad. Sci. U. S. A.* **95**:11875–11879.
11. Patrono, C., Coller, B., FitzGerald, G.A., Hirsh, J., and Roth, G. 2004. Platelet-active drugs: the relationships among dose, effectiveness, and side effects: the Seventh ACCP Conference on Antithrombotic and Thrombolytic Therapy. *Chest.* **126**(Suppl.):234S–264S.
12. Reilly, M., and FitzGerald, G.A. 2002. Gathering intelligence on antiplatelet drugs: the view from 30,000 feet. When combined with other information overviews lead to conviction. *Br. Med. J.* **324**:59–60.
13. Fitzgerald, D.J., Rocki, W., Murray, R., Mayo, G., and FitzGerald, G.A. 1990. Thromboxane A_2 synthesis in pregnancy-induced hypertension. *Lancet.* **335**:751–754.
14. Walsh, S.W. 1985. Preeclampsia: an imbalance in placental prostacyclin and thromboxane production. *Am. J. Obstet. Gynecol.* **152**:335–340.
15. Duley, L., Henderson-Smart, D.J., Knight, M., and King, J.F. 2004. Antiplatelet agents for preventing pre-eclampsia and its complications [review]. *Cochrane Database Syst. Rev.* 1:CD004659.
16. Chiaffarino, F., et al. 2004. A small randomised trial of low-dose aspirin in women at high risk of pre-eclampsia. *Eur. J. Obstet. Gynecol. Reprod. Biol.* **112**:142–144.
17. Walsh, S.W. 2004. Eicosanoids in preeclampsia. *Prostaglandins Leukot. Essent. Fatty Acids.* **70**:223–232.
18. FitzGerald, G.A., et al. 1983. Endogenous biosynthesis of prostacyclin and thromboxane and platelet function during chronic administration of aspirin in man. *J. Clin. Invest.* **71**:676–688.
19. Carmeliet, P., et al. 1996. Abnormal blood vessel development and lethality in embryos lacking a single VEGF allele. *Nature.* **380**:435–439.
20. Meyers, E.N., Lewandoski, M., and Martin, G.R. 1998. An Fgf8 mutant allelic series generated by Cre- and Flp-mediated recombination. *Nat. Genet.* **18**:136–141.
21. Nagy, A., et al. 1998. Dissecting the role of N-myc in development using a single targeting vector to generate a series of alleles. *Curr. Biol.* **8**:661–664.
22. Carlson, R.P., O'Neill-Davis, L., Chang, J., and Lewis, A.J. 1985. Modulation of mouse ear edema by cyclooxygenase and lipoxygenase inhibitors and other pharmacologic agents. *Agents Actions.* **17**:197–204.
23. Winyard, P.G., and Willoughby, D.A. 2003. Carageenan-induced paw edema in the rat and mouse. In *Inflammation protocols*. Humana Press. Totowa, New Jersey, USA. 115–123.
24. Patrignani, P., et al. 1999. COX-2 is not involved in thromboxane biosynthesis by activated human platelets. *J. Physiol. Pharmacol.* **50**:661–667.
25. Catella, F., and FitzGerald, G.A. 1987. Paired analysis of urinary thromboxane B_2 metabolites in humans. *Thromb. Res.* **47**:647–656.
26. Reilly, I.A., and FitzGerald, G.A. 1987. Inhibition of thromboxane formation in vivo and ex vivo: implications for therapy with platelet inhibitory drugs. *Blood.* **69**:180–186.
27. Catalano, P.M., Smith, J.B., and Murphy, S. 1981. Platelet recovery from aspirin inhibition in vivo; differing patterns under various assay conditions. *Blood.* **57**:99–105.
28. Darius, H., and Lefer, A.M. 1985. Blockade of thromboxane and the prevention of eicosanoid-induced sudden death in mice. *Proc. Soc. Exp. Biol. Med.* **180**:364–368.

29. Matsuno, H., Uematsu, T., Nagashima, S., and Nakashima, M. 1991. Photochemically induced thrombosis model in rat femoral artery and evaluation of effects of heparin and tissue-type plasminogen activator with use of this model. *J. Pharmacol. Methods.* **25**:303–317.
30. Gupta, D.K., Sato, T.A., Keelan, J.A., Marvin, K.W., and Mitchell, M.D. 2001. Expression of prostaglandin H synthase-1 and -2 in murine intrauterine and gestational tissues from mid pregnancy until term. *Prostaglandins Other Lipid Mediat.* **66**:17–25.
31. Horton, E.W., and Poyser, N.L. 1976. Uterine luteolytic hormone: a physiological role for prostaglandin $F_{2\alpha}$. *Physiol. Rev.* **56**:595–651.
32. Fuchs, A.R. 1995. Plasma membrane receptors regulating myometrial contractility and their hormonal modulation. *Semin. Perinatol.* **19**:15–30.
33. Fuchs, A.R., Fields, M.J., Freidman, S., Shemesh, M., and Ivell, R. 1995. Oxytocin and the timing of parturition. Influence of oxytocin receptor gene expression, oxytocin secretion, and oxytocin-induced prostaglandin F_2 and E_2 release. *Adv. Exp. Med. Biol.* **395**:405–420.
34. Riemer, R.K., and Heymann, M.A. 1998. Regulation of uterine smooth muscle function during gestation. *Pediatr. Res.* **44**:615–627.
35. Zingg, H.H., et al. 1995. Oxytocin and oxytocin receptor gene expression in the uterus. *Recent Prog. Horm. Res.* **50**:255–273.
36. Findlay, J.K. 1986. Angiogenesis in reproductive tissues. *J. Endocrinol.* **111**:357–366.
37. Vaskivuo, T.E., and Tapanainen, J.S. 2003. Apoptosis in the human ovary. *Reprod. Biomed. Online.* **6**:24–35.
38. McCracken, J.A., Schramm, W., Barcikowski. B., and Wilson, L., Jr. 1981. The identification of prostaglandin $F_{2\alpha}$ as a uterine luteolytic hormone and the hormonal control of its synthesis. *Acta Vet. Scand. Suppl.* **77**:71–88.
39. Arosh, J.A., et al. 2004. Prostaglandin biosynthesis, transport, and signaling in corpus luteum: a basis for autoregulation of luteal function. *Endocrinology.* **145**:2551–2560.
40. Ray, M.K., Fagan, S.P., and Brunicardi, F.C. 2000. The Cre-loxP system: a versatile tool for targeting genes in a cell- and stage-specific manner. *Cell Transplant.* **9**:805–815.
41. Lakso, M., et al. 1996. Efficient in vivo manipulation of mouse genomic sequences at the zygote stage. *Proc. Natl. Acad. Sci. U. S. A.* **93**:5860–5865.
42. Xu, X., et al. 2001. Direct removal in the mouse of a floxed neo gene from a three-loxP conditional knockout allele by two novel approaches. *Genesis.* **30**:1–6.
43. Kimura, T., et al. 1999. What knockout mice can tell us about parturition. *Rev. Reprod.* **42**:73–80.
44. Tsuboi, K., et al. 2000. Uterine expression of prostaglandin H2 synthase in late pregnancy and during parturition in prostaglandin F receptor-deficient mice. *Endocrinology.* **141**:315–324.
45. Tsuboi, K., Iwane, A., Nakazawa, S., Sugimoto, Y., and Ichikawa, A. 2003. Role of prostaglandin H2 synthase 2 in murine parturition: study on ovariectomy-induced parturition in prostaglandin F receptor-deficient mice. *Biol. Reprod.* **69**:195–201.
46. Catella-Lawson, F., et al. 2001. Cyclooxygenase inhibitors and the antiplatelet effects of aspirin. *N. Engl. J. Med.* **345**:1809–1817.
47. McAdam, B.F., et al. 2000. Effect of regulated expression of human cyclooxygenase isoforms on eicosanoid and isoeicosanoid production in inflammation. *J. Clin. Invest.* **105**:1473–1482.
48. Schonbeck, U., Sukhova, G.K., Graber, P., Coulter, S., and Libby, P. 1999. Augmented expression of cyclooxygenase-2 in human atherosclerotic lesions. *Am. J. Pathol.* **155**:1281–1291.
49. Cyrus, T., et al. 2002. Effect of low-dose aspirin on vascular inflammation, plaque stability, and atherogenesis in low-density lipoprotein receptor-deficient mice. *Circulation.* **106**:1282–1287.
50. Rocca, B., et al. 2000. Directed vascular expression of the thromboxane A_2 receptor results in intrauterine growth retardation. *Nat. Med.* **6**:219–221.
51. Tiano, H., et al. 2002. Deficiency of cyclooxygenase-1 or cyclooxygenase-2 alters epidermal differentiation and reduces mouse skin tumorigenesis. *Cancer Res.* **62**:3395–3401.
52. Chulada, P.C., et al. 2000. Genetic disruption of Ptgs-1, as well as of Ptgs-2, reduces intestinal tumorigenesis in Min mice. *Cancer Res.* **60**:4705–4708.
53. Akunda, J.K., et al. 2004. Genetic deficiency or pharmacological inhibition of cyclooxygenase-1 or -2 induces mouse keratinocyte differentiation in vitro and in vivo. *FASEB J.* **18**:185–187.
54. Asanuma, M., Miyazaki, I., and Ogawa, N. 2004. Neuroprotective effects of nonsteroidal anti-inflammatory drugs on neurodegenerative diseases. *Curr. Pharm. Des.* **10**:695–700.
55. Tybulewicz, V.L., Crawford, C.E., Jackson, P.K., Bronson, R.T., and Mulligan, R.C. 1991. Neonatal lethality and lymphopenia in mice with a homozygous disruption of the c-abl proto-oncogene. *Cell.* **65**:1153–1163.
56. Chen, X.S., Sheller, J.R., Johnson, E.N., and Funk, C.D. 1994. Role of leukotrienes revealed by targeted disruption of the 5-lipoxygenase gene. *Nature.* **372**:179–182.
57. Sun, D., and Funk, C.D. 1996. Disruption of 12/15-lipoxygenase expression in peritoneal macrophages. Enhanced utilization of the 5-lipoxygenase pathway and diminished oxidation of low density lipoprotein. *J. Biol. Chem.* **271**:24055–24062.
58. Knott, I., et al. 1993. Routine prostaglandin assay by GC-MS in multiwell tissue culture plates: application to human synoviocytes and chondrocytes. *Anal. Biochem.* **210**:360–365.
59. Bell-Parikh, L.C., et al. 2003. Biosynthesis of 15-deoxy-$\Delta^{12,14}$-PGJ_2 and the ligation of PPARγ. *J. Clin. Invest.* **112**:945–955. doi:10.1172/JCI200318012.
60. Dowd, N.P., Scully, M., Adderley, S.R., Cunningham, A.J., and Fitzgerald, D.J. 2001. Inhibition of cyclooxygenase-2 aggravates doxorubicin-mediated cardiac injury in vivo. *J. Clin. Invest.* **108**:585–590. doi:10.1172/JCI200111334.
61. Wade, R.L., Van Andel, R.A., Rice, S.G., Banka. C.L., and Dyer, C.A. 2002. Hepatic lipase deficiency attenuates mouse ovarian progesterone production leading to decreased ovulation and reduced litter size. *Biol. Reprod.* **66**:1076–1082.
62. Fowler, K.J., et al. 2004. Centromere protein b-null mice display decreasing reproductive performance through successive generations of breeding due to diminishing endometrial glands. *Reproduction.* **127**:367–377.